Journal of the Geological Society, *London*, Vol. **164**, 2007, pp. 87–97. Printed in Great Britain.

Episodic fire, runoff and deposition at the Palaeocene–Eocene boundary

M. E. COLLINSON[1], D. C. STEART[1], A. C. SCOTT[1], I. J. GLASSPOOL[2] & J. J. HOOKER[3]
[1]*Geology Department, Royal Holloway University of London, Egham TW20 0EX, UK (e-mail: D.steart@gl.rhul.ac.uk)*
[2]*Department of Geology, The Field Museum, 1400 S. Lake Shore Drive, Chicago, IL 60605-2496, USA*
[3]*Palaeontology Department, Natural History Museum, Cromwell Road, London SW7 SBD, UK*

Abstract: Qualitative and quantitative coal petrological analyses have been undertaken on the laminated lignite at the base of the Cobham Lignite Bed, from Scalers Hill, Kent, England. The maximum negative carbon isotope excursion, which marks the beginning of the Palaeocene–Eocene thermal maximum (PETM), occurs near the top of the laminated lignite. The lignite contains inertinite, a petrographic term used to describe charcoal. The laminated lignite has inertinite-rich and inertinite-poor layers indicative of episodic fires and post-fire erosion. Charcoal clasts are derived from living or recently senesced plants and are dominated by the leaf stalks of herbaceous ferns and wood fragments from flowering plants. The charcoal assemblage reflects a low-diversity flora, possibly adapted to disturbance by fire, derived from a source vegetation subjected to seasonal surface wildfires. The environmental conditions leading up to and across the onset of the PETM are, therefore, interpreted as incorporating a persistent fire regime with episodic wildfires followed by rainfall and runoff events. Abundant charcoal indicates near-modern oxygen levels whereas the absence of charred peat in this area calls into question previous suggestions that burning of Palaeocene peats might have contributed to the short-lived negative carbon isotope excursion at the Palaeocene–Eocene boundary.

The Palaeocene–Eocene boundary is marked by the onset of a period of enhanced greenhouse warming, with a significant mid- to high-latitude temperature increase of 4–6 °C lasting <220 ka (Bains *et al*. 1999; Norris & Röhl 1999; Röhl *et al*. 2000; Harrington 2001; Harrington *et al*. 2005). This event, termed the Palaeocene–Eocene thermal maximum (PETM), is characterized by a negative stable carbon isotope excursion (CIE), which indicates that large amounts of isotopically light carbon were released into the global atmosphere (Dickens 1999; Katz *et al*. 1999; Norris & Röhl 1999; Thomas *et al*. 1999; Harrington 2001). It is widely thought that in excess of 2×10^{12} tonnes of isotopically light carbon were released by the destabilization of continental shelf deposits containing methane gas hydrates, a mass of greenhouse gases sufficient to induce this significant but short-lived climate change event (Katz *et al*. 2001; Zachos *et al*. 2005).

The Cobham Lignite Bed provides a rare terrestrial record of the effect of the PETM on mid-latitude vegetation (Collinson *et al*. 2003). This lignite sequence (Fig. 1), located in Kent, England, occurs in a small outlier of Palaeogene strata in the eastern London Basin. It overlies the upper Palaeocene Upnor Formation and underlies the lower Eocene Woolwich Shell Beds (Woolwich Formation). The key biostratigraphic, magnetostratigraphic and sequence stratigraphic markers, including the negative CIE associated with the Palaeocene–Eocene boundary, which date this lignite, have been described by Collinson *et al*. (2003).

Organic deposits immediately underlying the lower Woolwich Shell Beds are frequently present within the outcrop area of the Woolwich Formation and one also occurs within the laterally interdigitating Reading Formation (Collinson *et al*. 2003). However, such deposits are normally either only a few centimetres thick, as at Swanscombe (Skipper 1999), or occur as thin intercalations within thicker muds, as at Newhaven (Dupuis & Gruas-Cavagnetto 1985) and Sidcup (Brown & Wrigley 1925; personal observation by M.E.C. and J.J.H.). The Cobham outlier is unusual in showing a thickness of lignite increasing from 0.15 m at the western outcrop edge (Chandler 1923; Martin 1976) to 2 m at Scaler's Hill, the study site. The apparently very localized thickening, together with minor faulting in the underlying sand and mud unit, suggests a locally subsiding area at Cobham. Although the exact geometry is unknown, the evidence (fine lamination, little to no clastic input and that only of mud grain size) suggests the presence of a shallow still water body such as a coastal plain lake. The widespread occurrence of organic deposits underlying the Woolwich Shell Beds, in some areas overlying channelling sands, suggests that they represent base-level rise over a flood plain low in a transgressive systems tract (Skipper 1999), specifically sequence Th5 (Hardenbol *et al*. 1998; Collinson *et al*. 2003).

The Cobham Lignite Bed (Fig. 1) is divided into a lower laminated part (Fig. 2a and b) up to 55 cm thick, studied herein, in which the CIE onset occurs, and an overlying blocky part (Collinson *et al*. 2003). The 2 m thick succession offers a considerably expanded sequence in which to detect floristic and environmental change immediately prior to and during the PETM. Penecontemporaneous floras close to the Palaeocene–Eocene transition in southern England, such as from Felpham (West Sussex), St. Pancras (central London) and Croydon (Surrey), suggest that the prevailing vegetation was mesothermal in character, whereas floras of the early Eocene climatic optimum reflect a paratropical megathermal vegetation with coastal mangroves, dominated by the palm *Nypa* (Collinson & Cleal 2001; Collinson *et al*. 2003).

Inertinite is a petrographic term used to describe fossil charcoal, and can be considered synonymous with it (Jones 1993; Scott 1989, 2000, 2002; Scott & Glasspool 2006). Herein, the terms inertinite and charcoal are used as is appropriate to the context, the term inertinite being favoured when referring to charcoal viewed in reflected light. Inertinite reflectance under oil

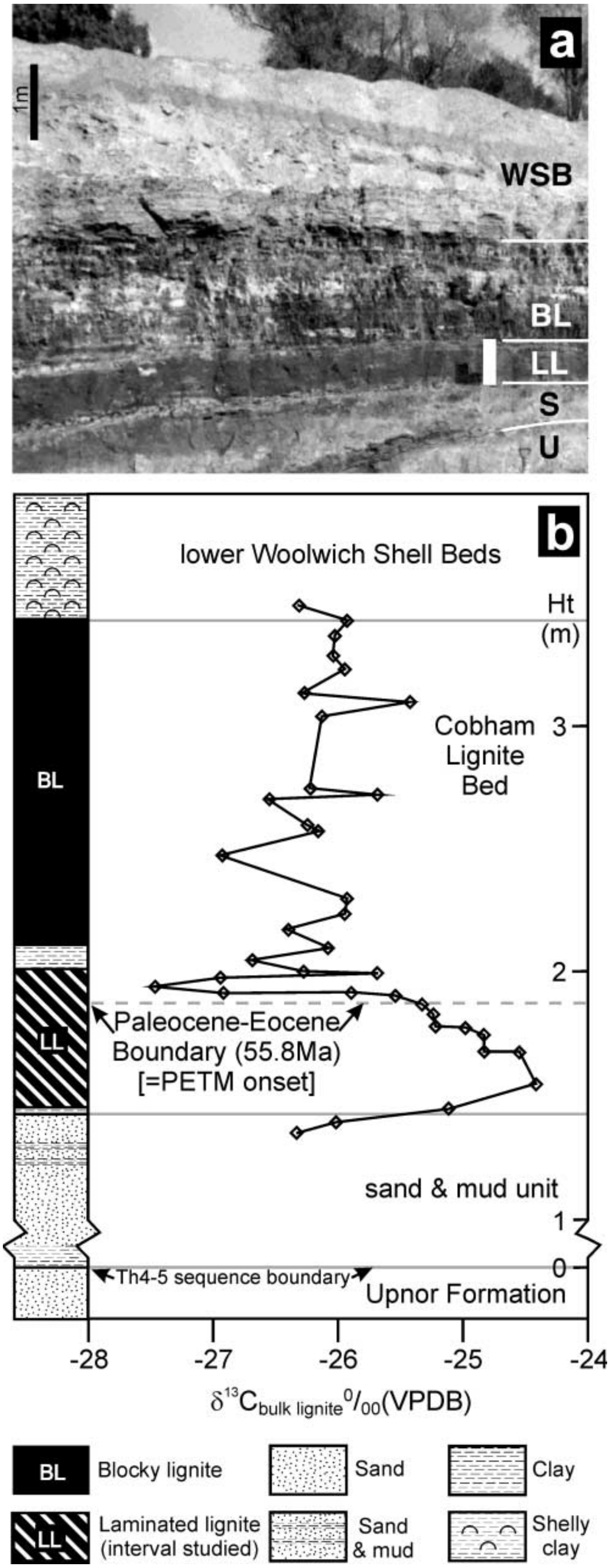

Fig. 1. The Cobham Lignite Bed at Scalers Hill, Cobham, Kent, UK, showing the laminated lignite unit studied herein. (**a**) Field photograph showing the main stratigraphic units. WSB, Woolwich Shell Beds; BL, Cobham Lignite Bed with blocky lignite; LL, Cobham Lignite Bed with laminated lignite; S, sand and mud unit; U, Upnor Formation. White bar indicates the unit studied (i.e. the laminated lignite). Scale bar represents 1 m. (b) Stratigraphic context of the Cobham Lignite Bed (including the laminated lignite (LL) studied herein), in a lithological log of Upnor Formation (base not seen) to basal shell beds of the Woolwich Formation. The Palaeocene–Eocene boundary date is from Gradstein *et al*. (2004). The Upnor Formation–sand and mud unit junction is incised, marking the Th4–5 sequence boundary (Collinson *et al*. 2003) and predating the Palaeocene–Eocene boundary by *c*. 80 ka (Hardenbol *et al*. 1998). The *Apectodinium* acme (a proxy for the PETM interval in paralic and marine environments; see Collinson *et al*. (2003) for discussion) is recorded from the lower Woolwich Shell Beds at the nearby site of Upnor, Kent (Powell *et al*. 1996), in the Jubilee Line 404T borehole, London (Ellison *et al*. 1996) and at Newhaven, East Sussex (Dupuis & Gruas-Cavagnetto 1985).

increases with both the temperature and duration of heating (Jones *et al*. 1991; Scott & Glasspool 2005). The lower laminated part of the Cobham Lignite Bed contains both fine and coarser charcoal clasts (Collinson *et al*. 2003), and therefore has the potential to reveal the local fire regime before and during the onset of the PETM. A number of papers have described how charcoal is produced during, and transported following, wildfire events (e.g. Clark *et al*. 1998; Pitkänen *et al*. 1999; Nichols *et al*. 2000; Ohlson & Tryterud 2000; Lynch *et al*. 2004). These studies have shown that particles less than 20 μm in diameter are typically transported by wind whereas those larger than 200 μm are typically not. In situations where particles larger than 200 μm do occur in sediments, it is likely that they were transported to the depositional setting via hydraulic flow. A combination of small and large particles is more likely to indicate a local fire, as extensive water transport selects for different-sized particles based upon their buoyancy and sedimentation characteristics (Nichols *et al*. 2000).

Ancient wildfires not only produce well-preserved charcoalified plant materials, they also serve as an indicator of general climatic variables, modify the structure of the source vegetation, and may affect the global carbon balance (Flannigan *et al*. 2000; Pyne *et al*. 1996; Schmidt & Noack 2000; Scott 2000). For example, McKenzie *et al*. (2004) stated that fire return intervals in the Holocene were shorter during periods of warmer, drier climate and Scott *et al*. (2000*b*) indicated that *c*. 8×10^9 tonnes of vegetation are burned naturally by wildfire each year. The occurrence of woody v. herbaceous plant materials in a fossil locality also provides information on the fire frequency. Frequent fire return intervals (1–3 years) tend to promote vegetation dominated by herbaceous plant species, whereas woody plant species tend to favour lower to rare fire frequencies (Mueller-Dombois & Goldammer 1990; Bond & van Wilgen 1996; Hoffmann 1999; Heisler *et al*. 2004).

Kurtz *et al*. (2003) posited that the rapid burning of accumulated Palaeocene terrestrial organic carbon, especially in peatlands, may have contributed to the negative carbon isotope excursion at the Palaeocene–Eocene boundary. Those workers argued that this burning could have been on a scale sufficient to cause the PETM event and that this mechanism serves as an alternative explanation to the release of marine carbon.

This paper aims to document the nature and distribution of inertinite in the laminated lignite (the lower unit of the Cobham Lignite Bed), which includes the maximum negative CIE and hence the onset of the PETM. Polished blocks of lignite studied using coal petrological methods allowed observation of inertinite *in situ*, and provided a permanent record of the sample for future reference. These data on inertinites are used to reconstruct the production, transport and depositional history of the charcoal, to interpret the fire regime, and to determine the biological nature and source community of the burnt material. This evidence also contributes to the understanding of causal factors implicated in the carbon isotope excursion and to reconstruction of palaeo-environmental conditions immediately prior to, and during, the onset of the PETM.

Materials and methods

Preparation, microscopy and photo-microscopy

Plaster jacketed blocks (columns between 10 cm × 10 cm and 20 cm × 20 cm in cross-section) of lignite collected in the field (see Collinson *et al*. 2003, for details) were cut in half. One half was retained for future study (Fig. 2a). The other half was subdivided into manageable coherent overlapping sequences and cleaned in preparation for resin embedding. The samples were then oven dried under vacuum at 50 °C for 5 h, then at 60 °C overnight. After cooling, Epofix resin was dribbled over the samples and allowed to cure. This resin penetrated through the lignite, stabilizing it, and allowed the blocks to be manipulated for subsequent embedding in polyester resin. Once fully cured, the samples were ground with a coarse grit paper (80 Grit), and then reimpregnated with polyester resin. The blocks were again cured and then dry ground with sequentially finer sandpapers (240 Grit, 1200 Grit and 2400 Grit) until ready for polishing. Finally, the samples were polished on unnapped cloths using 9, 6, 3 and 1 μm diamond pastes in sequence. Repeat surface resin impregnation and polishing was undertaken as necessary. All polishing and cutting was undertaken without water to prevent swelling and destruction of the lignite.

The polished blocks (example shown in Fig. 2b) were examined in reflected light under oil using either a Nikon Optiphot or Microphot reflected light microscope with either ×20 or ×40 oil immersion objectives. Most work was conducted using the ×20 objective; clast sizes were determined with a Whipple Grid that had a 35 μm grid spacing at this magnification. Subsidiary fluorescence microscopy used the Nikon Microphot reflected light microscope and a Nikon HB10101AF super high pressure mercury lamp fitted with an EX450-490 excitation filter, and a BA520 barrier filter. Photomicrographs were gathered as 24 bit JPEG greyscale images with a microscope-mounted Nikon digital sight DS-5M camera head and DS-L1 controller with either 1280 × 960 or 2560 × 1920 pixel resolution. Photomontage work, necessary for the imaging of the larger clasts and microstratigraphy, often used up to 60 separate images, and was completed using Corel Photo-Paint™ Version 11 or 12.

Coal petrology: inertinite quantification

Inertinite quantification was undertaken using a 100 point counting system. The maceral classification scheme used was based on International Committee for Coal and Organic Petrology (2001), and Scott & Glasspool (2006). The principal subcategories of inertinite were scored (i.e. fusinite, semifusinite, inertodetrinite, macrinite and micrinite), as well as two additional categories: ‘mineral’ grains (including pyrite) and ‘other’, which included all other organic materials not belonging to the inertinite maceral group (i.e. huminite and liptinite). The count used a standard 10 column by 10 row eyepiece Whipple Grid at ×200 magnification and was undertaken on a Nikon Microphot reflected light microscope with a Nikon LS 101 fibre optic light source. The maceral type at each Whipple Grid vertex was classified and recorded until 100 points were counted. Vertex points covering resin-filled cavities were not counted. Counts were taken of individual lithotypes, which were subdivided either by distinct maceral changes or, where more uniform, subtle changes in the maceral composition. Where possible, counts were repeated 10 times (giving 1000 points) to allow statistical analysis. Statistical analyses of the point counts were undertaken using Microsoft

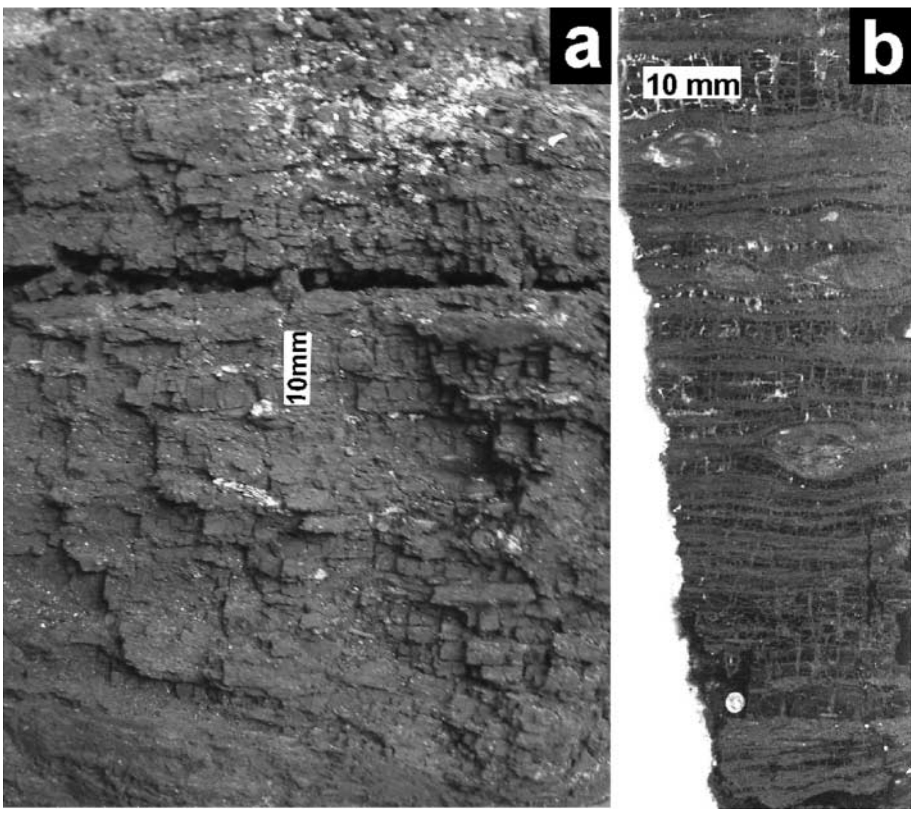

Fig. 2. (**a**) Plaster-jacketed portion of the laminated lignite, before embedding, showing layering. (**b**) Representative resin-embedded polished block photographed prior to the final polish, showing the millimetre-scale layering that occurs throughout the laminated lignite. The lighter layers are inertinite-rich, and the darker layers are inertinite-poor but huminite-rich. (Refer to Fig. 6 for microscopic detail.) The left of the image shows the plaster jacket. Scale bar in both (**a**) and (**b**) represents 10 mm.

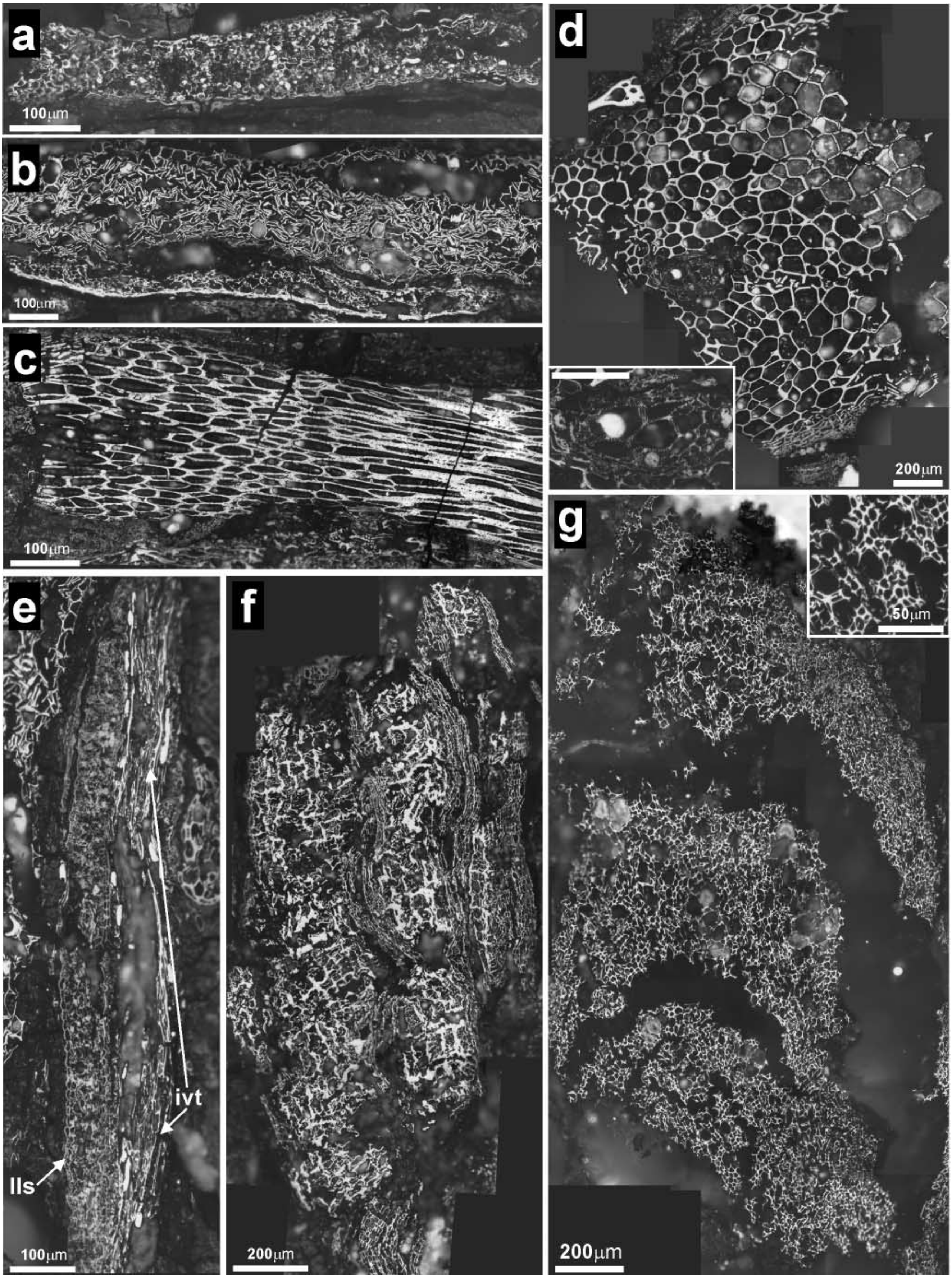
a
100µm
b
100µm
c
100µm
d
200µm
e
ivt
lls
100µm
f
200µm
g
50µm
200µm

Excel™ and programmed formulae for standard error derived from Zar (1999).

The rank of the lignite was determined using standard vitrinite reflectance procedures (Taylor *et al*. 1998). Huminite reflectance was quantified under oil of refractive index 1.518 at 23 °C, using light filtered to 546 nm, against Silica Glass, Spinel and YAG, calibration standards with reflectances of 0.038%, 0.393% and 0.929%, respectively.

Results

The vitrinite reflectance confirms the low rank of the laminated lignite (R_0 0.39 ± SD 0.1%). The inertinite (= fossil charcoal) found in the laminated lignite occurred either as discrete clasts, or as inertinite-rich layers ranging in thickness from less than 20 μm to over 500 μm. Often, but not always, these inertinite-rich layers were separated by inertinite-poor layers that were equally variable in thickness. Rare spores and pollen were occasionally recognized under fluorescence microscopy. No fluorescing cuticle was observed. Pyrite framboids occurred throughout the block. Individual inertinite-rich layers across the block varied from short (up to 3 mm) and narrowly lenticular (up to 200 μm thick), to those that could be tracked across the full width of the block (Fig. 2b). Often shorter layers contained one or two larger inertinite clasts (mostly of the inertinite maceral fusinite), with numerous smaller inertinite fragments of variable reflectance. Clasts with recognizable cellular structure were not uniform in their distribution, state of preservation, completeness, size, orientation or reflectance.

Inertinite (charcoal) clast size and orientation

The range of clast sizes was highly variable, from large well-preserved examples (mostly plant axes) with excellent anatomical detail, in excess of 1500 μm in diameter, to individual cells, cell fragments and inertodetrinite fragments less than 5 μm in their longest dimension. Clasts over 1500 μm occurred throughout the lignite sequence but were rarer than clasts between 200 and 1500 μm, which were common throughout. Clasts between 50 and 200 μm in diameter were numerous, and particles below this size were very abundant. The lignite as a whole contained the full size range of inertinite clasts mentioned above, but some layers contained specific size categories (see below). In the polished blocks, charcoalified plant organs were seen in transverse section (e.g. Fig. 3a, b, d, e, 'lls'; Fig. 4a-c, e, f), longitudinal section (Fig. 3e, 'ivt'; Fig. 4d) and in oblique section (Fig. 3c). The bedding and lamination surfaces clearly demonstrate that there was no particular orientation (Fig. 5) of the inertinite clasts.

Inertinite (charcoal) distribution

The distribution of inertinite clasts through the lignite was not uniform. The differences in inertinite occurrence are shown graphically in the bar charts in Figure 6, where T.I. represents total inertinite, T.O. represents total other organic (e.g. huminite), and T.M. represents total mineral.

The first category of inertinite distribution consisted mostly of inertinite-poor areas (Fig. 6a) where only scattered small fragments of inertodetrinite exist in a dark grey huminite background, interspersed with occasional inertinite-rich layers. In places, the areas that are inertinite-poor exhibit microlaminations of coal macerals (predominantly huminite) on a 10–30 μm scale. Inertinite percentages averaged around 9% (± SD 4.8; SE 1.7) for the inertinite-poor layers (e.g. Fig. 6a, bands a–c) and around 50% (± SD 5.1; SE 1.6) for the inertinite-rich layers (e.g. Fig. 6a, b and d).

The second type of inertinite distribution consisted of alternating layers of inertinite-rich and inertinite-poor lignite of variable thickness. Layers were identified by having clear lateral continuity across the block, and by a composition that was different from that of the layer above and below. These layers can be on a *c*. 100 μm scale and typically, this scale of layering occurred as repeating pairs of alternating inertinite-rich (54% ± SD 13.1; SE 4.2; Fig. 6b, bands a, c, e and g) and inertinite-poor (21% ± SD 9.7; SE 3.2; Fig. 6b, bands b, d and f) lignite. The inertinite-poor layers are similar to those described above and shown in Figure 6a. The inertinite-rich layers can be much thicker, ranging from 500 μm to more than 1 mm (Fig. 6c, band b). The total inertinite fraction in these thick inertinite-rich layers can be highly variable, averaging 47% (± SD 17.4; SE 5.4). The polished blocks (Fig. 2b) clearly reveal these thick inertinite-rich layers, which confer the hand-specimen fracture properties characteristic of the laminated lignite as shown in Figure 2a.

Botanical affinity

Most clasts over 150 μm in size were of a sufficient size and anatomical detail to indicate the category of botanical organ to which they belonged (i.e. stem, leaf stalk, leaf, wood, etc.), as well as their high-level taxonomic identity (i.e. angiosperm, pteridophyte, etc.). Almost all the specimens encountered were either herbaceous (Figs 3b, c, d and 4a, c, e), or woody (Figs 3f, g and 4b) stem axes or leaf stalks. Rare leaf-lamina-like structures were also found (Fig. 3a and e, 'lls'). Only two major plant groups, herbaceous ferns (pteridophytes) and woody (and possibly herbaceous) dicotyledonous flowering plants (angiosperms) have been identified. No material with obvious gymnosperm, monocot, bryophyte, algal or fungal affinities was identified, and no diaspores, flowers or roots were found in the laminated lignite. Fluorescence microscopy was used to search for non-charred fluorescing material (e.g. cuticles, algal cell walls) but, apart from rare spores and pollen, no fluorescing material was observed.

The charcoalified herbaceous material is represented mostly by plant axes (here, the term 'axes' includes fern leaf stalks). Figure 3d shows a large herbaceous axis, with a single intact vascular bundle. The vascular bundle has perforation plates between the vessel elements, and vascular tissue with scalariform thickenings (see inset in Fig. 3d). The presence of vessel elements with perforation plates without secondary growth indicates that this specimen was either a herbaceous angiosperm or pteridophyte axis, as both ferns and angiosperms have vessel elements (Carlquist & Schneider 2001). It is most probably a fern leaf stalk, as it has a single central vascular bundle, a characteristic of the extremities of fern rachides, not the radial arrangement of multiple vascular bundles typical of angiosperms. However, as a part of the axis is missing, this diagnosis is not absolutely

Fig. 3. Examples of the major charcoal clast types found in the Cobham laminated lignite, seen in reflected light under oil. (**a**) Possible leaf lamina in transverse section; (**b**) crushed axis tissue in transverse section; (**c**) oblique longitudinal section of herbaceous nonvascular tissue with 'checking'; (**d**) herbaceous axis with vascular bundle in transverse section (inset shows detail of vascular tissue; scale bar is 100 μm); (**e**) possible leaf lamina (lls) in transverse section, with unrelated elongate vascular strand (ivt) alongside; (**f**) periderm clast; (**g**) highly fractured diffuse porous angiosperm wood (inset shows detail of vessels and fibres).

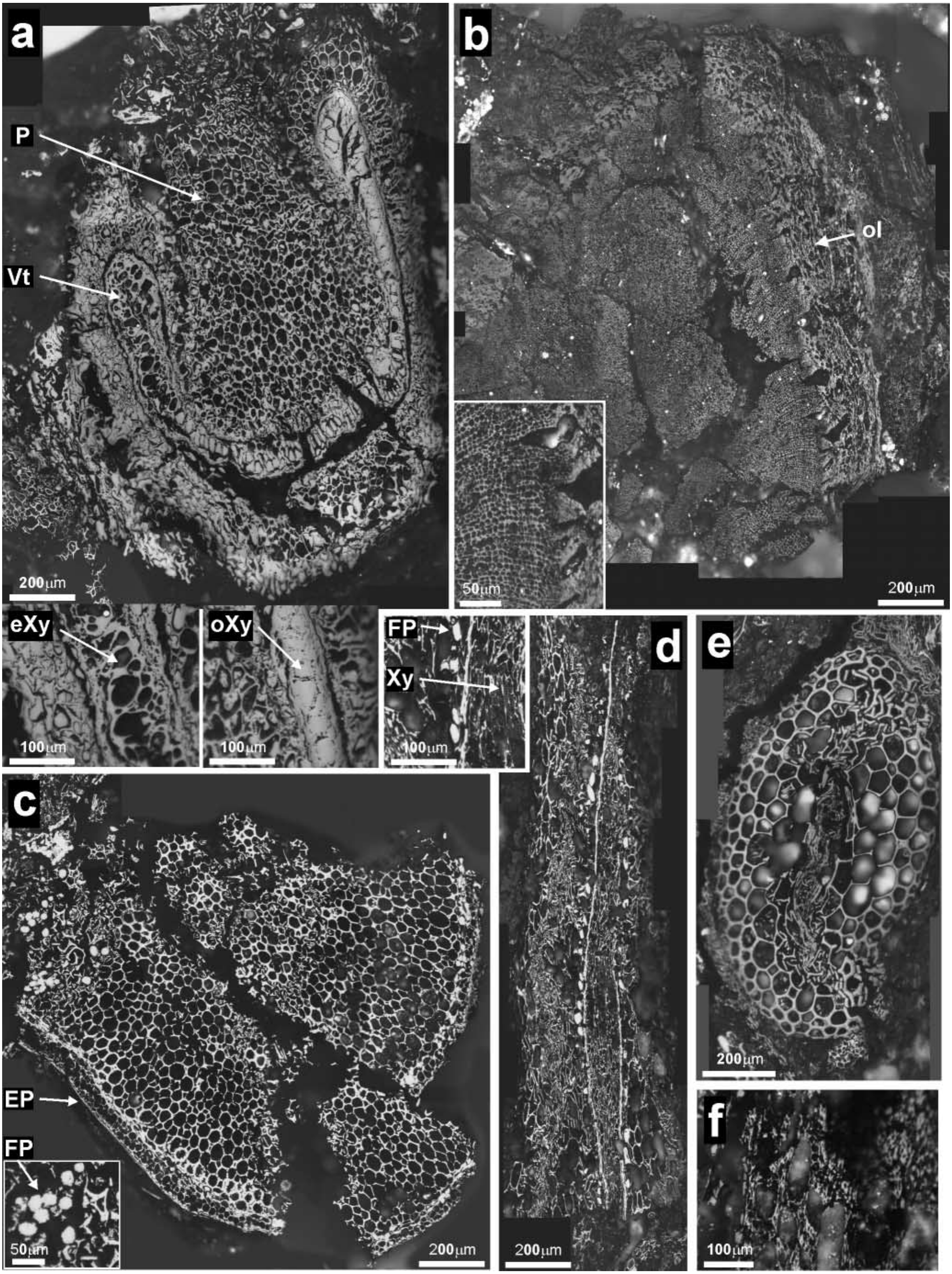
a
P
Vt
200µm
b
ol
50µm
200µm
eXy
100µm
oXy
100µm
FP
Xy
100µm
d
e
c
EP
FP
50µm
200µm
200µm
200µm
f
100µm

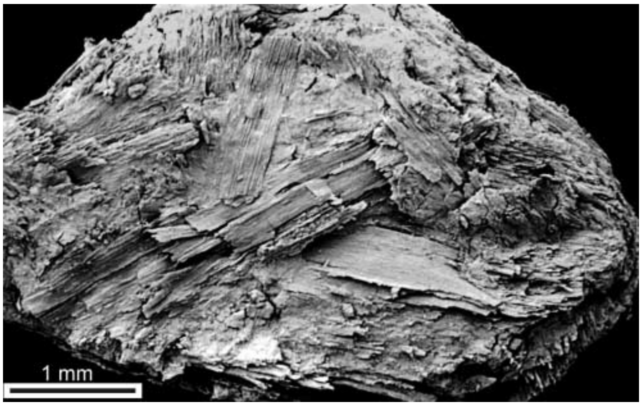

Fig. 5. Scanning electron micrograph of a fragment of the laminated lignite, broken approximately along a lamina surface. The charred clasts have a clear random orientation.

beyond doubt. The smaller specimen shown in Figure 4e also shows a herbaceous (probably fern) axis, although it is much smaller than the one in Figure 3d, and also has the remains of a partially crushed vascular bundle running through it.

The specimen in Figure 4a depicts a particularly well-preserved fern rachis in transverse section whose gross anatomy and cell detail is largely intact throughout the clast. It is a high-reflectance clast in which the vascular tissue (Fig. 4a, 'vt') and ground parenchyma (Fig. 4a, 'p') tissue can be easily discerned. The specimen has the typical U-shaped meristele exhibited by many fern species (Tansley 1908; Sporne 1975; Collinson & Ribbins 1977; Kramer & Green 1993; Collinson 2001). The level of cellular detail preserved in this specimen is high, with details of the vascular perforation plates being visible, even though some of the cell lumina in the vascular tissue have high-reflectance infills. There appears to be a separation of the vascular tissue (meristele) away from the parenchymatous ground tissue. This may have happened in the early stages of senescence or in the early stages of charring. Many of the cells towards the outside of the specimen (except those at the top) seem to have undergone modification, possibly indicating senescence. The cells towards the top have been shattered but not crushed.

Charred herbaceous specimens that have been compacted and fractured are common throughout the lignite. The specimen in Figure 3b is a typical example, where the cell walls have collapsed on top of each other as they shattered, forming tightly packed masses or stacks of cell-wall fragments. The degree of compaction in this specimen is such that it lacks sufficient anatomical detail to positively assign either its organ type or high-level taxonomy, although it was probably a herbaceous axis. Figure 3b can be compared with the more intact specimens of the same tissue type shown in Figure 4c and e, where the presence of vascular and parenchymatous tissue (Fig. 4e) and the relationships between the various cell fragments (Fig. 4c and e) are intact enough to indicate that they are herbaceous axes.

There are also numerous clasts, such as that shown in Figure 4c, that have excellent anatomical preservation, but whose diagnostic information is too limited to infer their taxonomic identity with certainty. The latter specimen has a clear epidermis (Fig. 4c, 'EP'), and a large mass of parenchymatous tissue. The absence of vascular tissue limits the potential diagnostic information, although it was a herbaceous plant axis and the similarity to Figure 3d suggests a fern leaf stalk. Charred faecal pellets occur in Figure 4c (FP) and in Figure 4d. These are rare, and occur in clasts with cellular anatomy preserved. They may indicate arthropod feeding on living or very recently senescent tissue.

Clasts of charred angiosperm wood are scattered throughout the block. These clasts occur in a wide range of sizes, one of the larger examples being shown in Figure 3g and one of the smallest in Figure 4f. The specimen in Figure 3g has no particular concentration of vessel elements in one part of the clast compared with another, supporting a diagnosis of diffuse porous wood. The cellular anatomy of the clast in Figure 3f has alternating layers of large and small diameter cells, and is interpreted as a periderm (bark) clast.

The large clast in Figure 4b has cells with considerably narrower lumina than those in Figure 3g, but they do exhibit some variation in size (see inset, Fig. 4b). This specimen is thus interpreted as angiosperm wood, as there is too much variation in cell sizes for it to be gymnosperm wood (Fahn 1967; Schweingruber 1990). Furthermore, Collinson *et al*. (2003) examined many wood clasts and their wall pitting under the scanning electron microscope and found no pitting characteristic of gymnosperm wood. The outermost layer of this specimen (Fig. 4b, 'ol') has periderm preserved.

Two examples of probable leaf tissue are shown (Fig. 3a and e, 'lls'), the only examples we have encountered. Epidermal and mesophyll (but not palisade mesophyll) cells can be observed in both these specimens, but there is no distinct cuticle (as determined by fluorescence microscopy). Neither of these specimens had stomatal apertures, so they may represent some other laminar plant organ, such as a scale (e.g. a fern leaf stalk scale, or a flowering plant bud scale).

Fig. 4. Examples of the major charcoal clast types found in the Cobham laminated lignite, seen in reflected light under oil. (**a**) Fern rachis in transverse section with crushing towards top; Vt, vascular tissue; P, parenchyma. Inset: eXy, xylem with empty lumen; oXy, xylem with occluded lumen. (**b**) Putative angiosperm wood with large-scale fracturing. ol, outer layer of periderm. Inset shows a detail of boundary of wood and periderm. (**c**) Herbaceous axis, with epidermis (EP) and faecal pellets (FP), with detail shown in inset. (**d**) Herbaceous axis (probably fern) in longitudinal section. Inset: FP, faecal pellets; Xy, xylem cells. (**e**) Small herbaceous axis (possibly fern) in transverse section. (**f**) Angiosperm wood with large vessels.

Discussion

The inertinite macerals, as identified in reflected light under oil, are generally considered to represent fossil charcoal and are the product of wildfire (Scott 2000, 2002; Scott & Glasspool 2006). Charred particles produced from wildfire may be transported by wind or water (Clark 1988; Nichols *et al*. 2000). In the Cobham laminated lignite, the occurrences of scattered small particles ($<$5–10 μm) of inertodetrinite in the absence of larger inertinite clasts (fusinite and semifusinite) are strongly suggestive of airborne transport and deposition of charcoal, possibly linked to regional fires (Clark 1988; Clark *et al*. 1998). Conversely, inertinite-rich layers contain large inertinite clasts ($>$200 μm). The random orientation and angular shape of these larger clasts, and their co-occurrence with smaller particles, argues against long-distance transport and sorting of charcoal (Nichols *et al*. 2000; Scott 2000), and suggests that the larger clasts were produced during local fires in the source vegetation.

Rainfall following fire may give rise to extensive erosion, and sediment may be transported from the burnt areas into a range of sedimentary systems such as rivers and lakes (Swanson 1981;

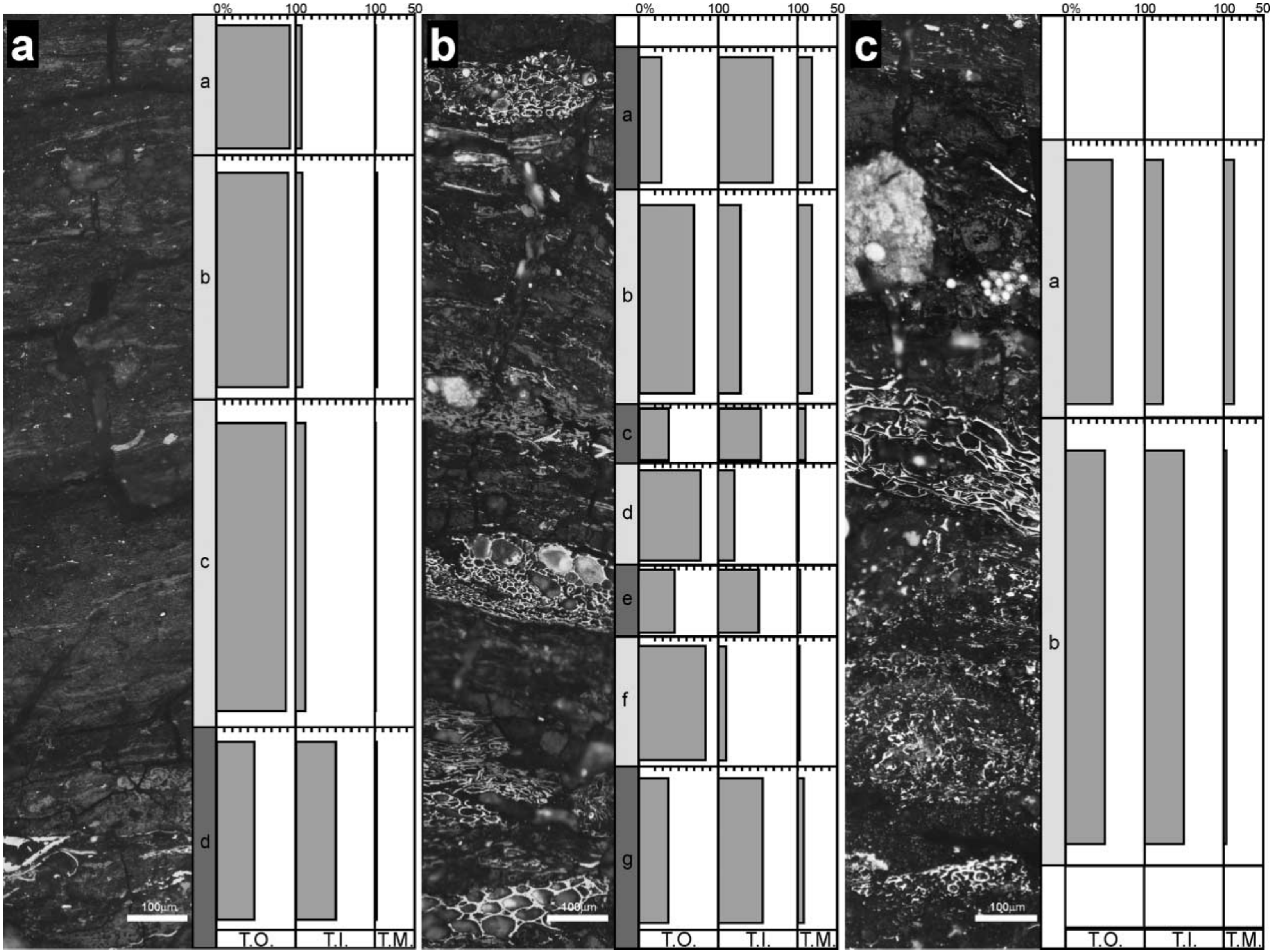

Fig. 6. Lignite in polished blocks imaged using reflectance microscopy under oil, showing the different types of inertinite distribution observed in the laminated lignite and the results of the maceral point counts. Scale bars represent 100 µm. T.M., total mineral; T.I., total inertinite, including fusinite, semifusinite, micrinite, inertodetrinite and macrinite; T.O, total other organic material. (**a**) An inertinite-poor interval (bands a–c), containing exclusively scattered inertodetrinite, with microlamination of coal macerals in places. At the base there is an inertinite-rich layer (band d). (**b**) Alternating fine-scale inertinite-rich (bands a, c, e, g) and inertinite-poor layers (bands b, d, f). (**c**) At base (band b), a thick (millimetre-scale) inertinite-rich layer containing various maceral fractions. (Refer to Fig. 2b for macroscopic image of inertinite-rich–inertinite-poor layering.)

Meyer *et al*. 1992; Millspaugh & Whitlock 1995; Whitlock & Millspaugh 1996; Martin & Moody 2001; Moody & Martin 2001; Robichaud & Elsenbeer 2001). The inertinite-rich–inertinite-poor inertinite layering may be linked to episodic fires and post-fire erosion events. The thickest (millimetre-scale) inertinite-rich layers may reflect single local fire events, as the accumulation of large volumes of charcoal particles, between 0.2 and 1.5 mm in diameter, often appears to indicate local fire events (Clark 1988; Lynch *et al*. 2004). The smaller-scale (*c*. 100 μm) fine alternating inertinite-rich and inertinite-poor layers indicate episodic and possibly even periodic runoff events of varying intensity. Larger clasts could have been mobilized by higher-intensity rainfall events over locally burned areas. In addition, this scale of layering may also reflect episodic local runoff where slow-moving thin sheets of surface water, formed during gentle precipitation, lift the smallest charcoal fragments and transport them to the depositional setting.

Inertinite-poor layers with exclusively inertodetrinite probably record more regional background fire events, as the occurrence of particles whose size range is <5–20 μm in diameter, without the presence of larger (>500 μm) particles, indicates airborne transport (Clark 1988; Ohlson & Tryterud 2000). Further, Clark (1988) indicated that 5–10 μm charcoal fragments do not begin to be deposited for about a kilometre from the combustion source and can remain suspended for many kilometres, particularly if the fire's convection column reaches great height. Alternatively, the inertinite-poor layers may reflect low-intensity post-fire runoff events with or without the input of airborne micro-charcoal.

It is more difficult to comment on fire frequency in the vegetation that formed this lignite. That the fire regime must have been episodic is evident, as the alternating inertinite-rich and inertinite-poor layers indicate this. It is not possible to say whether the fire regime was seasonal (i.e. annual), or longer term and more episodic. The presence of charred angiosperm wood throughout the lignite sequence tends to suggest a fire regime with a period greater than 3 years, possibly of the order of tens of years, as many woody angiosperms require more than one growth season to persist in the vegetation and complete their life cycles, particularly if they are fire sensitive (Mueller-Dombois & Goldammer 1990; Bond & van Wilgen 1996; Hoffman 1999; Heisler *et al*. 2004).

The majority of the charred clasts appear to be derived from herbaceous plants, especially ferns, with rarer examples of flowering plant wood. The charcoalified clasts of both ferns and dicotyledonous angiosperms suggest that these two groups of plants were the major components in the source vegetation. It has been shown that a charcoal assemblage that has undergone little transport may reflect the taxonomic composition of the source vegetation (Scott *et al*. 2000*a*). The plants from Cobham contrast with those from other contemporaneous English coastal region localities such as Felpham, where perennial monocots (palms) were a major local component of the vegetation (Collinson & Cleal 2001; Collinson *et al*. 2003). The absence of perennial monocots, combined with the absence of gymnosperms, suggests a low-diversity flora possibly adapted to disturbance by fire. This is supported by the preliminary palynology data reported by Collinson *et al*. (2003), which showed that members of the angiosperm families Juglandaceae and Betulaceae were present in the vegetation, along with ferns that produced *Cicatricosisporites* spores. No gymnosperm pollen was recorded.

The well-preserved, mostly anatomically complete, clasts show that either living or very recently dead (senescent) biomass was burned. Altered cell walls and cell infills (possibly related to decay) occur throughout the laminated lignite but are rare. There is no evidence of charring of any original peat surface. Had such charring occurred, then one would expect masses of either structureless pyrolytic carbon, or lignite with concentrated inertodetrinite resulting from the slow heating associated with peat burning (Peterson 1998). This argues against ground fires (Pyne *et al*. 1996; Scott *et al*. 2000*a*), the products of which should also include charcoalified peat and charcoalified decayed litter. This casts doubt upon the hypothetical widespread peatland fires proposed by Kurtz *et al*. (2003) as a possible cause of the PETM carbon stable isotope excursion.

There is a limited diversity of plant organs represented as charcoal. There are very few if any leaf laminae, no disseminules, flowers or roots, but charcoalified axes and fern leaf stalks. This indicates that it was the aerial organs of the plants that were burning. The laminar portion of thin, delicate laminate leaves of both ferns and flowering plants might be prone to complete combustion. However, charcoalified flowers, fruits and seeds are well known as fossils (Scott 2000), and are also found in modern charcoal deposits (Scott *et al*. 2000*a*), and charred fern reproductive structures have also been reported (Gandolfo *et al*. 1997; Collinson *et al*. 2000; Collinson 2002). Therefore, the absence of charred plant reproductive organs suggests that fires might have occurred in a season (e.g. dry winter–spring) when reproductive structures had not been produced. This further supports fire episodicity and hints at distinct fire seasons. The rarity of charcoalified leaf laminae is consistent with crown or surface fires where the laminar portions of leaves have been consumed by burning. We can see no reason why fern leaf stalks and woody twigs of similar size would be differentially sorted by current transport. Therefore, the relative rarity of wood and high abundance of herbaceous material (including fern leaf stalks) suggests that this was not a forest through which only a crown fire could have burned, and argues in favour of surface fires consuming herbaceous low-growing plants including ferns.

Collectively these data indicate production of charcoal by episodic surface fires and certainly not by the burning of decayed litter such as would occur in soils or by burning of peat. The episodic runoff and depositional events recorded in the laminated Cobham lignite deposit are typical of modern systems where rainfall occurs following extensive surface fires (Robichaud & Waldrop 1994; Robichaud & Elsenbeer 2001; Graham 2003).

Our results show that there is abundant charcoal in the laminated lignite immediately before and across the Palaeocene–Eocene boundary. Earlier Palaeocene lignites also contain high levels of inertinite (Potter *et al*. 1991; Demchuk 1993; Hackley *et al*. 2005). These data support the recent model (Berner 2006) of near-modern oxygen levels between 18.5 and 19.8% for 50–70 Ma.

Conclusions

The vegetation surrounding the accumulating Cobham laminated lignite experienced fire on both regional and local scales. Episodic fires and post-fire erosion events are reflected in the inertinite (= charcoal) distribution in the lignite. The majority of the charred clasts are derived from herbaceous plants, especially ferns, with rarer examples of flowering plant wood. This suggests a low-diversity flora possibly adapted to disturbance by fire. The absence of charcoalified peat and of charcoalified decayed litter is indicative of surface or crown fires. The presence of herbaceous aerial organs, but absence of bryophytes and fungi and relative rarity of wood suggests surface fires. The absence of reproductive organs further supports fire episodicity by suggesting fire seasonality.

The environmental conditions in this area leading up to and across the initiation of the PETM event are interpreted as incorporating a persistent fire regime comprising regular drier intervals with surface fires followed by rainfall and runoff events. Furthermore, this study adds significantly to the very limited data for early Cenozoic records of charcoalified plant material. The fire regime, with abundant charcoal, shows that oxygen levels immediately preceding and at the onset of the PETM must be near modern. There is no evidence of Palaeocene burned peat at this locality, indicating that the model proposed by Kurtz *et al.* (2003), which suggests that the rapid burning of accumulated Palaeocene peat deposits was a major contributor to the carbon isotope excursion, is open to question. However, if fire regimes similar to that observed in the Cobham laminated lignite were widespread across mid-latitude regions, then this has implications for the release of isotopically light carbon, potentially contributing to the carbon isotope excursion and associated climate change.

The authors would like to thank Alfred McAlpine, AMEC and Channel Tunnel Rail Link for access to the Cobham Lignite Bed, S. Rose for making arrangements, the Leverhulme Trust for providing the funding (Grant Number F/07/537/0) that made this project possible, and J. Skipper and S. Tracey for help with initial sample collection and field discussions. We are grateful to S. Hesselbo, I. Harding and J. Marshall, for their constructive reviews and comments that helped to improve the paper. We would also like to thank personnel from the Geology Department, Royal Holloway University of London, for their support, especially N. Holloway (assistance with sample polishing and preparation), S. Gibbons (Palaeobiology laboratory) and K. D'Souza (photomicrography). This is a contribution to Natural History Museum research framework, focus number 2.

References

Bains, S., Corfield, R.M. & Norris, R.D. 1999. Mechanism of climate warming at the end of the Paleocene. *Science*, **285**, 724–727.

Berner, R.A. 2006. GEOCARBSULF: a combined model for Phanerozoic atmospheric O_2 and CO_2. *Geochimica et Cosmochimica Acta*, in press.

Bond, W.J. & van Wilgen, B.W. 1996. *Fire and Plants*. Chapman and Hall, London.

Brown, E.E.S. & Wrigley, A. 1925. Notes on the sections exposed in the Sidcup by-pass road. *Proceedings of the Geologists' Association*, **36**, 76–79.

Carlquist, S. & Schneider, E.L. 2001. Vessels in ferns: structural, ecological and evolutionary significance. *American Journal of Botany*, **88**, 1–13.

Chandler, R.H. 1923. The Tertiary section at Shorne Wood, Cobham, Kent. *Proceedings of the Geologists' Association*, **34**, 137–141.

Clark, J.S. 1988. Particle size motion and the theory of charcoal analysis: source area, transport, deposition and sampling. *Quaternary Research*, **30**, 67–80.

Clark, J.S., Lynch, J., Stocks, B.J. & Goldammer, J.G. 1998. Relationships between charcoal particles in air and sediments in west–central Siberia. *Holocene*, **8**, 19–29.

Collinson, M.E. 2001. Cainozoic ferns and their distribution. *Brittonia*, **53**, 173–235.

Collinson, M.E. 2002. The ecology of Cainozoic ferns. *Review of Palaeobotany and Palynology*, **119**, 51–68.

Collinson, M.E. & Cleal, C.J. 2001. The palaeobotany of the Palaeocene and Palaeocene–Eocene transitional strata in Great Britain. *In:* Cleal, C.J., Thomas, B.A., Batten, D.J. & Collinson, M.E. (eds) *Mesozoic and Tertiary Palaeobotany of Great Britain*. Joint Nature Conservation Committee, Peterborough, Geological Conservation Review Series, **22**, 164–168.

Collinson, M.E. & Ribbins, M.M. 1977. Pyritised fern rachides in the London Clay. *Tertiary Research*, **1**, 109–113.

Collinson, M.E., Featherstone, C., Cripps, J.A., Nichols, G.J. & Scott, A.C. 2000. Charcoal-rich plant debris accumulations in the lower Cretaceous of the Isle of Wight, England. *Acta Palaeobotanica, Supplement*, **2**, 93–105.

Collinson, M.E., Hooker, J.J. & Gröcke, D.R. 2003. Cobham Lignite bed and penecontemporaneous macrofloras of southern England: a record of vegetation and fire across the Paleocene–Eocene Thermal Maximum. *In:* Wing, S.L., Gingerich, P.D., Schmitz, B. & Thomas, E. (eds) *Causes and Consequences of Globally Warm Climates in the Early Paleogene*. Geological Society of America, Special Papers, **369**, 333–349.

Demchuk, T.D. 1993. Petrology of fibrous coal (fusain) and associated inertinites from the Early Paleocene of the central Alberta Plains. *International Journal of Coal Geology*, **24**, 211–232.

Dickens, G.R. 1999. The blast from the past. *Nature*, **401**, 752–755.

Dupuis, C. & Gruas-Cavagnetto, C. 1985. Les Woolwich Beds et le London Clay de Newhaven (East Sussex), données palynologiques et stratigraphiques nouvelles. *Bulletin d'Information des Géologues du Bassin de Paris*, **22**, 19–33.

Ellison, R.A., Ali, J.R., Hine, N.M. & Jolley, D.W. 1996. Recognition of Chron C25n in the Upper Paleocene Upnor Formation of the London Basin, UK. *In:* Knox, R.W.O'B., Corfield, R.M. & Dunay, R.E. (eds) *Correlation of the Early Paleogene in Northwest Europe*. Geological Society, London, Special Publications, **101**, 185–193.

Fahn, A. 1967. *Plant Anatomy*. Pergamon, Oxford.

Flannigan, M.D., Stocks, B.J. & Wotton, B.M. 2000. Climate change and forest fires. *Science of the Total Environment*, **262**, 221–229.

Gandolfo, M.A., Nixon, K.C., Crepet, W.L. & Ratcliffe, G.E. 1997. A new fossil fern assignable to Gleicheniaceae from Late Cretaceous sediments of New Jersey. *American Journal of Botany*, **84**, 483–493.

Gradstein, F.M., Ogg, J.G. & Smith, A.G. et al. 2004. *A Geologic Time Scale 2004*. Cambridge University Press, Cambridge.

Graham, R.T. (ed.) 2003. *Hayman fire case study*. US Department of Agriculture, Forest Service, Rocky Mountain Research Station, Ogden, UT, General Technical Report, **RMRS-GTR-114**.

Hackley, P.C., Warwick, P.D. & González, E. 2005. Petrology, mineralogy and geochemistry of mined coals, western Venezuela. *International Journal of Coal Geology*, **63**, 68–97.

Hardenbol, J., Thierry, J., Farley, M.B., Jacquin, T., De Graciansky, P.C. & Vail, P.R. 1998. Mesozoic and Cenozoic sequence chronostratigraphic framework of European basins. *In:* de Graciansky, P.-C., Hardenbol, J., Jaquin, T. & Vail, P.R. (eds) *Mesozoic and Cenozoic Sequence Stratigraphy of European Basins*. SEPM (Society for Sedimentary Geology), Special Publications, **60**, 3-13, 763-781.

Harrington, G.J. 2001. Impact of Paleocene/Eocene greenhouse warming on North American paratropical forests. *Palaios*, **16**, 266–278.

Harrington, G.J., Clechenko, E.R. & Clay Kelly, D. 2005. Palynology and organic carbon isotope ratio across a terrestrial Palaeocene/Eocene boundary section in the Williston Basin, North Dakota, USA. *Palaeogeography, Palaeoclimatology, Palaeoecology*, **226**, 214–232.

Heisler, J.L., Briggs, J.M., Knapp, A.K., Blair, J.M. & Seery, A. 2004. Direct and indirect effects of fire on shrub density and aboveground productivity in a mesic grassland. *Ecology*, **85**, 2245–2257.

Hoffmann, W.A. 1999. Fire and population dynamics of woody plants in a neotropical savanna: matrix model projections. *Ecology*, **80**, 1354–1369.

International Committee for Coal and Organic Petrology (ICCP) 2001. The new inertinite classification (ICCP System 1994). *Fuel*, **80**, 459–471.

Jones, T.P. 1993. New morphological and chemical evidence for a wildfire origin for fusain from comparisons with modern charcoal. *Special Papers in Palaeontology*, **49**, 113-123.

Jones, T.P., Scott, A.C. & Cope, M. 1991. Reflectance measurements against temperature of formation for modern charcoals and their implications for the study of fusain. *Bulletin de la Société Géologique de France*, **162**, 193–200.

Katz, M.E., Pak, D.K., Dickens, G.R. & Miller, K.G. 1999. The source and fate of massive carbon input during the latest Paleocene thermal maximum. *Science*, **286**, 1531–1533.

Katz, M.E., Cramer, B.S., Mountain, G.S., Katz, S. & Miller, K.G. 2001. Uncorking the bottle: what triggered the Paleocene/Eocene thermal maximum methane release? *Paleoceanography*, **16**, 549–562.

Kramer, K.U. & Green, P.S. (eds) 1993. *Pteridophytes and Gymnosperms. The Families and Genera of Vascular Plants*. Springer, Berlin.

Kurtz, A.C., Kump, L.R., Arthur, M.A., Zachos, J.C. & Paytan, A. 2003. Early Cenozoic decoupling of the global carbon and sulfur cycles. *Paleoceanography*, **18**(4), 1090, doi:10.1029/2003PA000908.

Lynch, J.A., Clark, J.S. & Stocks, B.J. 2004. Charcoal production, dispersal, and deposition from the Fort Providence experimental fire: interpreting fire regimes from charcoal records in boreal forests. *Canadian Journal of Forest Research*, **34**, 1642–1656.

Martin, A.R.H. 1976. Upper Paleocene Salviniaceae from the Woolwich/Reading Beds near Cobham Kent. *Palaeontology*, **19**, 173–184.

Martin, D.A. & Moody, J.A. 2001. Post-fire, rainfall intensity–peak discharge relations for three mountainous watersheds in the western USA. *Hydrological Processes*, **15**, 2981–2993.

McKenzie, D., Gedalof, Z., Peterson, D.L. & Mote, P. 2004. Climatic change, wildfire, and conservation. *Conservation Biology*, **18**, 890–902.

Meyer, G.A., Wells, S.G., Balling, R.C. & Jull, A.J.T. 1992. Response of alluvial systems to fire and climate change in Yellowstone National Park. *Nature*, **357**, 147–150.

Millspaugh, S.H. & Whitlock, C. 1995. A 750-year fire history based on lake sediment records in central Yellowstone National Park, U.S.A. *Holocene*, **5**, 282–283.

Moody, J.A. & Martin, D.A. 2001. *Hydrological and sedimentologic response of two burned watersheds*. US Geological Survey Water-Resources Investigation Report, **01-4122**.

Mueller-Dombois, D. & Goldammer, J.G. 1990. Fire in tropical ecosystems and global environmental change: an introduction. *In:* Goldammer, J.G. (ed.) *Fire in the Tropical Biota: Ecosystem Processes and Global Challenges*. Ecological Studies, **84**, 1–10.

Nichols, G.J., Cripps, J.A., Collinson, M.E. & Scott, A.C. 2000. Experiments in water logging and sedimentology of charcoal: results and implications. *Palaeogeography, Palaeoclimatology, Palaeoecology*, **164**, 43–56.

Norris, R.D. & Röhl, U. 1999. Carbon cycling and chronology of climate warming during the Palaeocene/Eocene transition. *Nature*, **401**, 775.

Ohlson, M. & Tryterud, E. 2000. Interpretation of the charcoal record in forest soils: forest fires and their production and deposition of macroscopic charcoal. *Holocene*, **10**, 519–525.

Peterson, H.I. 1998. Morphology, formation and palaeo-environmental implications of naturally formed char particles in coals and carbonaceous mudstones. *Fuel*, **77**, 1177–1183.

Pitkänen, A., Lehtonen, H. & Huttunen, P. 1999. Comparison of sedimentary microscopic charcoal particle records in a small lake with dendrochronological data: evidence for the local origin of microscopic charcoal produced by forest fires of low intensity in eastern Finland. *Holocene*, **9**, 559–567.

Potter, J., Beaton, A.P., McDougall, W.J., Nambudiri, E.M.V. & Vigrass, L.W. 1991. Depositional environments of the Hart coal zone (Paleocene), Willow Bunch Coalfield, southern Saskatchewan, Canada from petrographic, palynological, paleobotanical, mineral and trace element studies. *International Journal of Coal Geology*, **19**, 253–281.

Powell, A.J., Brinkhuis, H. & Bujak, J.P. 1996. Upper Paleocene–lower Eocene dinoflagellate cyst sequence biostratigraphy of southeast England. *In:* Knox, R.W.O'B., Corfield, R.M. & Dunay, R.E. (eds) *Correlation of the Early Paleogene in Northwest Europe*. Geological Society, London, Special Publications, **101**, 145–183.

Pyne, S.J., Andrews, P.L. & Laven, R.D. 1996. *Introduction to Wildland Fire*. Wiley, New York.

Robichaud, P.R. & Elsenbeer, H. (eds) 2001. Wildfire and Superficial Processes. *Hydrological Processes*, **15**, 2865–3091.

Robichaud, P.R. & Waldrop, T.A. 1994. A comparison of surface runoff and sediment yields from low- and high-severity site preparation burns. *Water Resources Bulletin*, **30**, 27–34.

Röhl, U., Bralower, T.J., Norris, R.D. & Wefer, G. 2000. New chronology for the late Paleocene thermal maximum and its environmental implications. *Geology*, **28**, 927–930.

Schmidt, M.W.I. & Noack, A.G. 2000. Black carbon in soils and sediments: analysis, distribution, implications, and current challenges. *Global Biogeochemical Cycles*, **14**, 777–793.

Schweingruber, F.H. 1990. *Anatomy of European Woods*. Paul Haupt, Stuttgart.

Scott, A.C. 1989. Observations on the nature and origin of fusain. *International Journal of Coal Geology*, **12**, 443–475.

Scott, A.C. 2000. The Pre-Quaternary history of fire. *Palaeogeography, Palaeoclimatology, Palaeoecology*, **164**, 281–329.

Scott, A.C. 2002. Coal petrology and the origin of coal macerals: a way ahead? *International Journal of Coal Geology*, **50**, 119–134.

Scott, A.C. & Glasspool, I.J. 2005. Charcoal reflectance as a proxy for the emplacement temperature of pyroclastic flow deposits. *Geology*, **33**, 589–592.

Scott, A.C. & Glasspool, I.J. 2006. Observations and experiments on the origin and formation of inertinite macerals. *International Journal of Coal Geology*, in press.

Scott, A.C., Cripps, J., Nichols, G. & Collinson, M.E. 2000a. The taphonomy of charcoal following a Recent heathland fire and some implications for the interpretation of fossil charcoal deposits. *Palaeogeography, Palaeoclimatology, Palaeoecology*, **164**, 1–31.

Scott, A.C., Moore, J. & Brayshay, B. 2000b. Introduction to fire in the palaeoenviroment. *Palaeogeography, Palaeoclimatology, Palaeoecology*, **164**, vii–xi.

Skipper, J. 1999. *The stratigraphy of the Lambeth Group (Palaeocene) of South East England*. PhD thesis, London University.

Sporne, K.R. 1975. *The Morphology of Pteridophytes and Allied Plants: the Structure of Ferns and Allied Plants*, *4th*. Hutchinson, London.

Swanson, F.J. 1981. Fire and geomorphic processes. *In:* Mooney, H.A., Bonnicksen, T.H., Christensen, N.L., Lotan, J.E. & Reiner, W.A. (eds) *Fire Regimes and Ecosystem Properties*. US Department of Agriculture, Forest Service General Technical Report, **W026**, 401–420.

Tansley, A.G. 1908. *Lectures on the Evolution of the Filicinean Vascular System. New Phytologist. Reprint 2*. Cambridge University Press, Cambridge.

Taylor, G.H., Teichmüller, M., Davis, A., Diessel, C.F.K., Littke, R. & Robert, P. 1998. *Organic Petrology*. Borntraeger, Berlin.

Thomas, E., Zachos, J.C. & Bralower, T.J. 1999. Deep-sea environments in the absence of polar ice caps: the case of the Early Eocene. *In:* Huber, B.T., MacLeod, K.G. & Wing, S.L. (eds) *Warm Climates in Earth History.* Cambridge University Press, Cambridge, 132–160.

Whitlock, C. & Millspaugh, S.H. 1996. Testing the assumptions of fire-history studies: an examination of modern charcoal accumulations in Yellowstone National Park, U.S.AÒ *Holocene*, **6**, 7–15.

Zachos, J.C., Röhl, U. & Schellenberg, S.A. *et al.* 2005. Rapid acidification of the ocean during the Paleocene–Eocene thermal maximum. *Science*, **308**, 1611–1615.

Zar, J.H. 1999. *Biostatistical Analysis*. Prentice–Hall, Englewood Cliffs, NJ.

Received 16 December 2005; revised typescript accepted 16 May 2006.
Scientific editing by John Marshall